ORIGINAL ARTICLE

NMR analysis and chemical shift calculations of poly(lactic acid) dimer model compounds with different tacticities

Koto Suganuma[1,2], Ken Horiuchi[2], Hironori Matsuda[2], HN Cheng[3], Akihiro Aoki[1] and Tetsuo Asakura[1]

In this work, poly(lactic acid) (PLA) dimer model compounds with different tacticities were synthesized and studied in detail by ^1H and ^{13}C nuclear magnetic resonance (NMR) in three solvents, deuterated chloroform $(CDCl_3)/CCl_4$ (20/80 v/v), $CDCl_3$ and dimethyl sulfoxide -d_6. All of the peaks in the ^1H and ^{13}C NMR spectra were assigned with the help of two-dimensional NMR. Although the solvents were different, the tacticity splitting of the dimers showed no significant difference among the solvents. The chemical shifts were calculated and compared with experimental shifts to understand the origin of the tacticity splitting in PLA. Thus, a conformational energy calculation was first performed to determine the energetically stable states in isotactic and syndiotactic dimers by several quantum chemical calculation methods. The ^1H and ^{13}C chemical shifts were then calculated for each conformation of the model compounds by considering both the conformational energies of the predominant conformation and the chemical shift of each conformation. The observed tacticity splitting of the chemical shifts between isotactic and syndiotactic ^1H and ^{13}C NMR peaks of the dimers was reproduced particularly well, using the combination of Becke's three parameter hybrid method for conformational energy calculations and Hartree-Fock for chemical shift calculations.

INTRODUCTION

Poly(lactic acid) (PLA) is a well-known polymer that has been extensively studied.[1,2] Dimers, trimers and other oligomers of PLA usually occur in concentrated PLA solutions[3] and are useful materials in their own right, and have also been synthesized through polymerization[4–6] or degradation.[7] They can be used as building blocks for functional polymers, for example, oligomer-grafted dextran,[8] tetrafunctional oligomers[9] and oligomers encapped with sodium,[10] acrylates[11] and isocyanates.[12] In suitable cases, the oligomers may function as surfactants[10] and as substitutions for waxes, oils and other petroleum-based oligomers in commercial formulations (Futerro. Lactic acid oligomers. http://www.futerro.com/products_oligomers.html). In addition, they are useful as model compounds for PLA.

A major determinant of the physical properties of PLA is tacticity. Thus, mechanical properties and heat resistance have been reported to depend on tacticity.[13,14] Recently, it was shown that tacticity could influence thermal stability, T_m, T_g, crystallinity, solution stability and polymer degradability in star-shaped PLA.[15,16] In addition, poly (L-lactic acid) and poly(D-lactic acid) could form a 1/1 stereocomplex, and the crystalline structure of the stereocomplex was quite different from that of poly(L-lactic acid) or poly(D-lactic acid).[17–20] It was

reported that multiblock copolymers of poly(L-lactic acid) and poly(D-lactic acid) formed the stereocomplex more easily without first forming the single-polymer crystals.[21] However, PLA with short L- and D-block sequences exhibited relatively a low melting temperature.[22] Thus, it is important to have detailed information regarding PLA tacticity to understand and improve the polymer's physical properties.

Many nuclear magnetic resonance (NMR) studies of PLA tacticity, including two-dimensional NMR, have been reported using appropriate polymers and model compounds.[23–33] Most recently, we reported the calculation of ^1H and ^{13}C chemical shifts in PLA model compounds.[30] The ^1H and ^{13}C chemical shifts calculated with the quantum chemical method were compared with the observed chemical shifts, and good agreement was obtained for the relative chemical shifts of the ^1H and ^{13}C peaks of the CH group between isotactic and syndiotactic dimer model compounds.

Recent advances in quantum chemical calculations coupled with increases in computer speed and memory size have made it possible to predict the electronic structures of PLA and its model compounds more accurately.[34–37] Conformational analyses of PLA model compounds were reported[38,39] using a quantitative method, Becke's three parameter hybrid method (B3LYP)/6-31G (d,p), for

conformational energy calculations *in vacuo* or in the electronic environment within the condensed phase. Wu *et al.*[36] determined the equilibrium geometries, infra red, total energies and NMR chemical shifts of several lactides, including L-lactide, D-lactide and three *meso*-lactides, using several quantum chemical methods, such as B3LYP/6–311 + G(2d,p) and B3LYP/6–31G(d). Sadlej *et al.*[40] discussed the interaction energies, conformations, vibrational absorption and vibrational circular dichroism spectra for conformers of monomeric chiral D-lactic acid and their complexes with water using B3LYP/aug-cc-pVDZ and B3LYP/aug-cc-pVTZ.

In this work, the ^{1}H and ^{13}C NMR spectra of isotactic and syndiotactic PLA dimers are observed and assigned by two-dimensional NMR in several solvents to examine the influence of the solvents on tacticity splitting in the ^{1}H and ^{13}C NMR spectra. The chemical shift data in which solvent effects can be ignored are compared with the chemical shifts calculated using several quantum chemical methods. The calculations entail two independent steps using different quantum chemical methods, determining the conformational energy of the preferred conformation first, and then the chemical shifts for each preferred conformation. These calculations are examined with Hartree-Fock (HF) and B3LYP, because HF has been used more commonly in quantum chemical calculations and B3LYP has been used more commonly in density functional calculations. In general, the B3LYP method is effective in the calculation of the electron distribution state for the whole molecule, and HF is effective in calculating the local electron distribution state. The best combination of the quantum chemical methods is selected by virtue of the agreement between the calculated and the observed chemical shifts of the ^{1}H and ^{13}C nuclei of the CH groups of isotactic and syndiotactic dimer model compounds. The origin of the tacticity splitting in the NMR spectra of PLA is also discussed.

EXPERIMENTAL PROCEDURE
Synthesis of dimer model compounds (1) of PLA
The isotactic and syndiotactic dimer model compounds (**1**) (structure shown in Figure 1) were synthesized from (-)-O-acetyl-L-lactic acid and methyl S-(-)-lactate or R-(+)-lactate. The details of the synthesis and purification have been previously described.[30]

NMR measurement
^{1}H and ^{13}C NMR spectra were obtained on a JEOL α-600 spectrometer (JEOL, Tokyo, Japan) operating at 600 MHz and 150 MHz, respectively, at room temperature. Deuterated chloroform (CDCl$_3$), 80:20 (v/v) CCl$_4$:CDCl$_3$ and dimethyl sulfoxide (DMSO)-d$_6$ were used as solvents, and the sample concentration was 10% (w/v). The internal chemical shift reference was tetramethylsilane. The ^{1}H NMR spectra were obtained with a digital resolution of 0.36 Hz/point with 32 K data points, together with 45° flip angle and 4 s pulse delay. The ^{13}C NMR spectra were obtained with a digital resolution of 1.24 Hz/point with 32 K data points, together with a 45° flip angle and 2 s pulse delay. ^{1}H–^{13}C heteronuclear multiple bond correlation (HMBC) spectroscopy was performed using gradient pulse sequences. HMBC spectra were
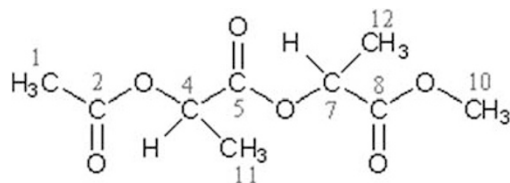
recorded for 7 h with a 60 ms delay for long-range ^{1}H–^{13}C coupling (^2J, ^3J, ^4J) selection, with spectral widths of 5.5 p.p.m. for ^{1}H, 250.0 p.p.m. for ^{13}C (all peaks), 38.6 p.p.m. for ^{13}C carbonyl or 34.7 p.p.m. for ^{13}C methyl. Before Fourier transformation, the free induction decays were zero-filled twice in the ^{13}C dimension, and a shifted sine bell function was applied to both dimensions.

Conformational energy calculation
The conformational energy calculation for the monomer model compound was carried out with the Gaussian 09 software program (Gaussian, Pittsburgh, PA, USA) as a function of the internal rotation angle. The quantum chemical method used was HF or B3LYP,[41] and the basis sets used were 6311 + G*,[42–44] TZVP[45–47] and cc-pVTZ.[48–52] The conformational energy calculation was also performed for isotactic and syndiotactic dimer model compounds for the preferred conformations selected from the Ramachandran map of the monomer model compound.

Chemical shift calculation
The magnetic shielding tensor was calculated quantum-chemically according to the GIAO method[53–58] for ^{1}H and ^{13}C nuclei of the two preferred conformations of the monomer model compound. The HF or B3LYP method was used, and the basis set was 6311 + G*, TZVP or cc-pVTZ. The isotropic chemical shifts were obtained for comparison with the observed chemical shifts. The ^{1}H and ^{13}C chemical shifts for tetramethylsilane were calculated using the same methods. For the ^{1}H and ^{13}C chemical shift calculations for dimer model compounds, a two-step procedure was used. In each model compound, the relative occurrence probabilities for the preferred conformations were first calculated by Boltzmann distribution, based on the difference in the conformational energies. Because the chemical shifts were calculated for each conformation quantum-chemically, the chemical shifts for each configuration were obtained by taking into account both the relative occurrence probability and the chemical shifts for each conformation.

RESULTS AND DISCUSSION
Assignment of ^{1}H and ^{13}C NMR spectra of PLA dimer model compounds
The ^{1}H and ^{13}C NMR spectra of isotactic and syndiotactic PLA dimer model compounds (**1**) were first obtained in CDCl$_3$. As expected, the ^{1}H and ^{13}C chemical shift difference between the two CH groups, 4 and 7 in Figure 1, was very small. The situation was similar for the

Figure 1 Dimer model compounds (**1**) of PLA. A full color version of this figure is available at *Polymer Journal* online.
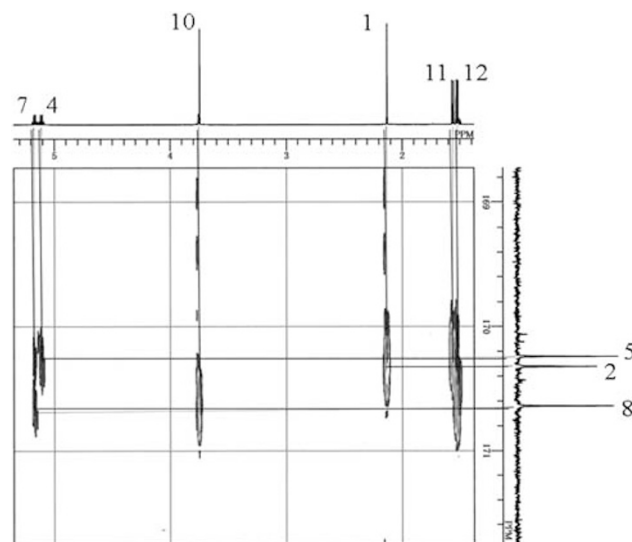

Figure 2 HMBC spectrum of isotactic dimer model compound of PLA in CDCl$_3$, expanded carbonyl region. A full color version of this figure is available at *Polymer Journal* online.

two CH$_3$ groups, 11 and 12, in Figure 1. Therefore, it is important to assign these peaks unambiguously. For this purpose, two-dimensional NMR was used, particularly the HMBC experiment, which provides ^{13}C–^{1}H multiple-bond correlations. The HMBC spectra of isotactic dimer model compound are shown in Figure 2 (carbonyl region), Figure 3 (methyl region) and Figure 4 (entire spectral region).

The peaks from H-1, H-10, C-1 and C-10 in Figure 1 were easily identified by their chemical shift values. Thus, the peaks at 2.1 p.p.m. and 20.6 p.p.m. were assigned to H-1 and C-1, and the peaks at 3.7 p.p.m. and 52.3 p.p.m. were assigned to H-10 and C-10, respectively. As shown in Figure 2, C-8 of carbonyl was assigned according to the correlations with H-10, and C-2 of carbonyl was assigned according to the correlations with H-1. Moreover, another carbonyl carbon was assigned to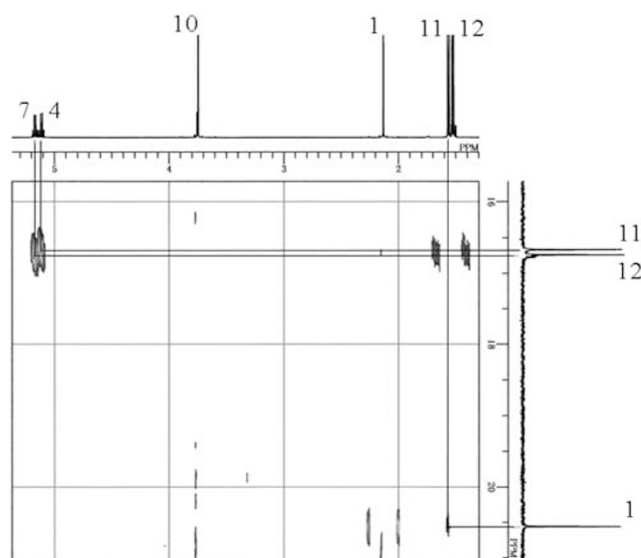 C-5. Two methine protons could be assigned according to the correlations with two carbonyl carbons, H-7 from C-8 and H-4 from C-5. Similarly, two methyl protons could be assigned according to the correlations with two carbonyl carbons, H-11 from C-5 and H-12 from C-8. The assignments of two methyl carbons were made according to the correlations shown in Figure 3. C-11 was assigned according to the correlations with H-4, and C-12 was assigned according to the correlations with H-7. Finally, the assignments of two methine carbons were made according to the correlations shown in Figure 4. C-4 was assigned according to the correlations with H-11, and C-7 was assigned according to the correlations with H-12. Similar assignments were achieved for the syndiotactic dimer model compound using the HMBC spectra (not shown). The chemical shifts and the assignments of the dimer model compounds observed in CDCl$_3$ are summarized in Table 1.

Figure 3 HMBC spectrum of isotactic dimer model compound of PLA in CDCl$_3$, expanded methyl region. A full color version of this figure is available at *Polymer Journal* online.
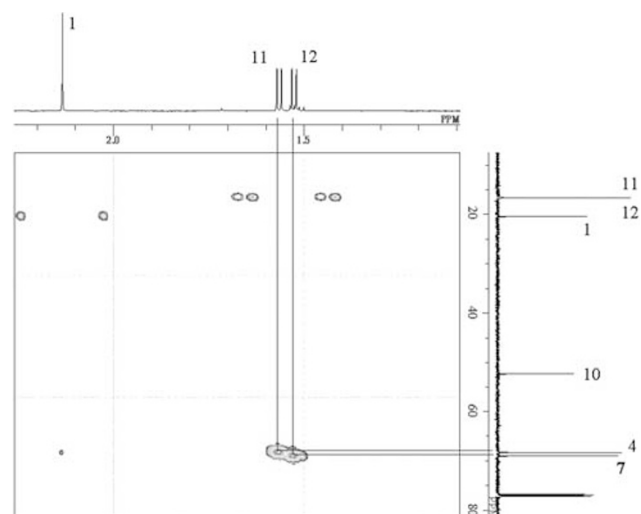

Figure 4 HMBC spectrum of isotactic dimer model compound of PLA in CDCl$_3$, entire spectral region. A full color version of this figure is available at *Polymer Journal* online.

Table 1 ^{1}H and ^{13}C chemical shifts (p.p.m. from TMS) of the isotactic and syndiotactic dimer model compounds (1) in several solvents

Type		Isotactic			Syndiotactic	
	CDCl$_3$/CCl$_4$			CDCl$_3$/CCl$_4$		
Solvent	(20/80 v/v)	CDCl$_3$	DMSO-d$_6$	(20/80 v/v)	CDCl$_3$	DMSO-d$_6$
^{1}H						
1	2.08	2.13	2.07	2.08	2.13	2.08
10	3.72	3.75	3.68	3.72	3.76	3.68
4	4.99	5.11	5.05	5.05	5.16	5.08
7	5.1	5.17	5.12	5.05	5.15	5.06
11	1.52	1.57	1.46	1.49	1.53	1.44
12	1.5	1.53	1.44	1.47	1.51	1.42
^{13}C						
1	20.21	20.55	20.27	20.23	20.56	20.29
10	51.91	52.32	52.29	51.94	52.38	52.23
4	68.01	68.3	68.04	68.17	68.44	68.2
7	68.56	69	68.95	68.81	69.14	69.09
11	16.54	16.68	16.52	16.64	16.77	16.58
12	16.65	16.75	16.56	16.65	16.8	16.61
2	169.53	170.33	170.05	169.35	170.14	169.87
5	169.26	170.24	169.87	169.12	170.08	169.82
8	169.99	170.65	170.39	169.78	170.44	170.29

Abbreviations: CDCl$_3$, deuterated chloroform; DMSO, dimethyl sulfoxide; TMS, tetramethylsilane.
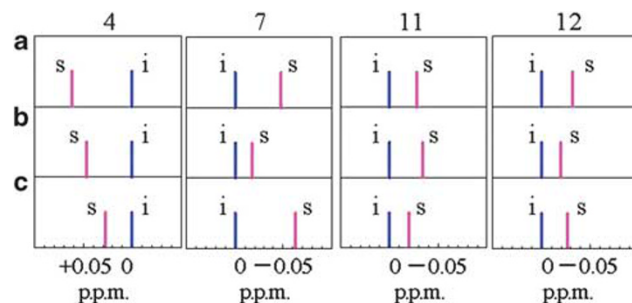

Figure 5 Comparison of the observed ^{1}H chemical shifts (in p.p.m.) of PLA dimer model compound (1) shown as stick spectra. The solvents are (a) CDCl$_3$/CCl$_4$ (20/80 v/v), (b) CDCl$_3$ and (c) DMSO-d$_6$. The chemical shifts are shown relative to the isotactic chemical shift. The blue stick corresponds to isotactic (i) and the pink stick to syndiotactic (s).

Effects of different solvents on the relative chemical shifts between isotactic and syndiotactic dimer model compounds

In the past, CDCl$_3$ and DMSO-d$_6$ were often used as NMR solvents for PLA. To compare the calculated and the observed chemical shifts, especially for tacticity splitting, the solvent effect should be minimized as much as possible, because chemical shift calculations are generally
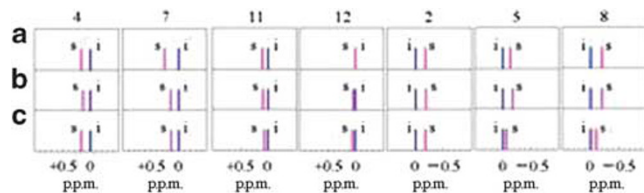

Figure 6 Comparison of the observed ^{13}C chemical shifts (in p.p.m.) of PLA dimer model compound (**1**) shown as stick spectra. The solvents are (**a**) CDCl$_3$/CCl$_4$ (20/80 v/v), (**b**) CDCl$_3$ and (**c**) DMSO-d$_6$. The chemical shifts are shown relative to the isotactic chemical shift. The blue stick corresponds to isotactic (i) and the pink stick to syndiotactic (s).

Table 2 The occurrence probabilities (%) of preferred conformations of dimer model compounds (**1**)

Type		Isotactic				Syndiotactic			
Method	Basis set	L1L1	L1L2	L2L1	L2L2	L2D1	L1D2	L1D1	L2D2
B3LYP	TZVP	77.31	17.51	3.1	2.08	45.08	30.64	12.96	11.33
HF	TZVP	86.3	12.16	0.83	0.7	52.48	28.91	10.63	7.98
B3LYP	cc-pVTZ	76.79	17.09	3.19	2.92	46.84	30.25	10.75	12.16
HF	cc-pVTZ	84.79	13.1	0.91	1.2	53.85	28.23	8.3	9.61
B3LYP	6311+G*	76.27	17.98	3.28	2.47	47.5	28.59	11.55	12.35
HF	6311+G*	84.13	13.9	0.87	1.11	53.87	27.82	8.73	9.58

performed on molecules *in vacuo*. It is well known that CDCl$_3$ is a polar solvent. It would be desirable to verify the effects of a less polar solvent and a more polar solvent on the relative chemical shifts between isotactic and syndiotactic dimer model compounds. DMSO-d$_6$ was selected because it is more polar than CDCl$_3$. A suitable non-polar solvent is CCl$_4$. PLA is insoluble, but the dimer model compounds are soluble in CCl$_4$. Thus, the solvent mixture CCl$_4$/CDCl$_3$ (20% v/v) was chosen, with 20% CDCl$_3$ added for ^{2}H field locking. For both of these solvents, unambiguous assignments were again required because of the small chemical shift differences between two CH groups and between two CH$_3$ groups in the dimer model compounds. The HMBC experiment was again conducted. The results for CDCl$_3$/CCl$_4$ (20/80 v/v) and DMSO-d$_6$ solvents are also presented in Table 1.

For ease of presentation, the observed chemical shifts for all ^{1}H and ^{13}C peaks of the dimer model compounds, except for those of two terminal CH$_3$ groups, are shown as stick spectra in Figures 5 and 6, respectively.

Note that the observed chemical shift differences are indeed very small between the isotactic and syndiotactic dimer model compounds for both ^{1}H and ^{13}C nuclei. However, there was no reversal of isotactic/syndiotactic assignments in different solvents. Moreover, there was no obvious trend between the chemical shift difference and solvent polarity. Thus, we can use the chemical shifts observed in CDCl$_3$/CCl$_4$ for comparison with the calculated chemical shifts.

Conformational energy calculations of the dimer model compounds (1)

The four energetically stable states generated from the combination of two preferred conformations in the Ramachandran conformational energy map of the monomer model compound[30] were the initial four preferred conformations of the dimer model compounds (**1**). The

Table 3 ^{1}H and ^{13}C chemical shifts (p.p.m. from TMS) of the isotactic dimer model compound (1) together with probability (%) of each conformation and observed chemical shifts in CDCl$_3$/CCl$_4$ (20/80 v/v)

Type	isotactic									
	Calculated									Observed
Code	(a)	(b)	(c)	(d)	(e)	(f)	(g)	(h)	(i)	(j)
Method and basis set of conformational optimization	B3LYP TZVP	B3LYP TZVP	HF TZVP	B3LYP cc-pVTZ	B3LYP cc-pVTZ	HF cc-pVTZ	B3LYP 6311+G*	B3LYP 6311+G*	HF 6311+G*	CDCl$_3$/CCl$_4$ (20/80 v/v)
Method and basis set of calculation of chemical shifts	HF TZVP	B3LYP TZVP	HF TZVP	HF cc-pVTZ	B3LYP cc-pVTZ	HF cc-pVTZ	HF 6311+G*	B3LYP 6311+G*	HF 6311+G*	
^{1}H										
4	4.48	4.84	4.28	5.14	5.55	4.98	4.71	4.99	4.53	4.99
7	4.57	4.92	4.32	5.26	5.65	5.05	4.76	5.02	4.55	5.1
11	1.56	1.52	1.51	2.02	2.01	2.01	1.62	1.56	1.58	1.52
12	1.46	1.43	1.39	1.94	1.94	1.92	1.53	1.49	1.47	1.5
^{13}C										
4	65.96	73.47	62.65	66.83	73.94	63.99	66.21	73.87	63.02	68.01
7	65.46	73.12	62.13	66.52	73.13	63.57	66.19	73.95	62.79	68.56
11	16.63	17.94	16.79	17.19	18.45	17.53	17.27	18.83	17.45	16.54
12	16.63	17.95	16.75	17.14	18.24	17.49	17.42	18.94	17.59	16.65
2	182.84	177.73	174.98	180.05	176.27	173.18	180.4	177.58	173.23	169.53
5	182.79	179.28	175.35	180.44	178.03	173.92	180	178.46	173.25	169.26
8	183.56	180.05	176.11	181.04	178.9	174.47	180.6	179.22	173.79	169.99

Abbreviations: CDCl$_3$, deuterated chloroform; TMS, tetramethylsilane.

Table 4 ^1H and ^{13}C chemical shifts (p.p.m. from TMS) of the syndiotactic dimer model compound (**1**) together with probability (%) of each conformation and observed chemical shifts in $CDCl_3/CCl_4$ (20/80 v/v)

Type	Syndiotactic									
	Calculated									Observed
Code	(a)	(b)	(C)	(d)	(e)	(f)	(g)	(h)	(i)	(j)
Method and basis set of conformational optimization	B3LYP TZVP	B3LYP TZVP	HF TZVP	B3LYP cc-pVTZ	B3LYP cc-pVTZ	HF cc-pVTZ	B3LYP 6311+G*	B3LYP 6311+G*	HF 6311+G*	CDCl₃/CCl₄ (20/80 v/v)
Method and basis set of calculation of chemical shifts	HF TZVP	B3LYP TZVP	HF TZVP	HF cc-pVTZ	B3LYP cc-pVTZ	HF cc-pVTZ	HF 6311+G*	B3LYP 6311+G*	HF 6311+G*	
^1H										
4	4.52	4.81	4.24	5.18	5.45	4.95	4.73	4.9	4.49	5.05
7	4.51	4.84	4.25	5.2	5.55	4.97	4.71	4.92	4.48	5.05
11	1.5	1.48	1.45	1.97	1.97	1.96	1.58	1.54	1.53	1.49
12	1.39	1.39	1.35	1.91	1.9	1.88	1.48	1.44	1.42	1.47
^{13}C										
4	66.22	75.12	63.52	67.85	75.44	65.55	67.13	75.51	64.5	68.17
7	66.09	73.12	62.76	66.83	73.61	63.72	66.37	74.08	62.87	68.81
11	17.05	18.16	17.1	17.59	18.6	17.91	17.61	19.05	17.71	16.64
12	16.58	17.99	16.68	17.14	18.28	17.41	17.47	18.96	17.56	16.65
2	182.8	177.59	174.99	180.02	176.23	173.2	180.39	177.49	173.28	169.35
5	182.68	178.46	175.19	180.35	177.47	173.78	180	177.95	173.26	169.12
8	183.28	179.45	175.83	180.8	178.37	174.24	180.33	178.87	173.57	169.78

Abbreviations: CDCl₃, deuterated chloroform; TMS, tetramethylsilane.

D-isomer of syndiotactic dimer model was derived by flipping the sign of the Z-coordinate of the X–Y–Z coordinates. The conformational energies of four conformations for each isotactic and syndiotactic dimer model compound (**1**) were optimized by two quantum chemical methods, B3LYP and HF, with different basis sets, that is, TZVP, cc-pVTZ and 6300+G*. The relative occurrence probabilities of the preferred conformations were calculated using a Boltzmann distribution and the difference in the conformational energies after optimization, as shown in Table 2. Here, the number '1' indicates the most stable conformation in the Ramachandran conformational energy map of the monomer model compound, and the number '2' indicates the second most stable conformation.

There is no abnormal trend among the occurrence probabilities of the preferred conformations calculated by different quantum chemical methods and different basis sets. However, there are significant differences between the values calculated by the B3LYP and HF methods. These differences seem to arise from the approximations used in the quantum chemical methods, because B3LYP includes electron correlation, but HF does not.

^1H and ^{13}C chemical shift calculations of dimer model compounds (1) and comparison between the calculated and observed chemical shifts

The ^1H and ^{13}C chemical shifts of each conformation of the dimer model compounds (**1**) were calculated and averaged by the occurrence probabilities. The chemical shifts of all ^1H and ^{13}C nuclei, except for those of two terminal CH_3 groups, are listed in Table 3 (isotactic) and Table 4 (syndiotactic), together with the observed chemical shifts in $CDCl_3/CCl_4$ (20/80 v/v).

The calculated and observed ^1H and ^{13}C chemical shifts are shown as stick spectra in Figures 7 and 8, respectively.
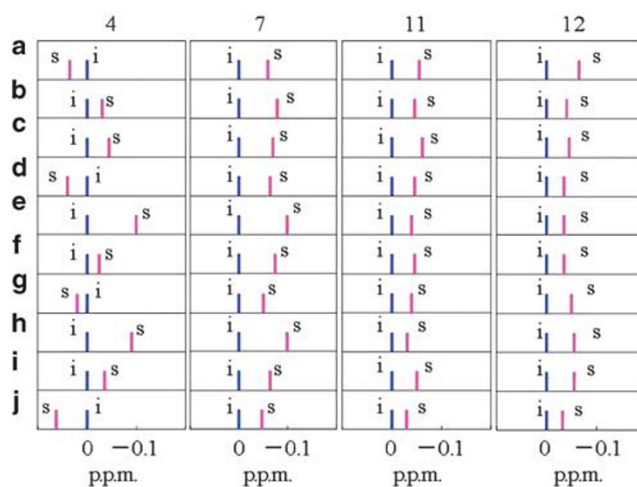

Figure 7 Comparison of calculated and observed ^1H chemical shifts (in p.p.m.) of PLA dimer model compounds (**1**) shown as stick spectra. (a–i) represent the calculated chemical shift, (j) represents the observed chemical shift. The identity of each code is presented in row 3 of Tables 3 and 4. The chemical shifts are shown relative to the isotactic chemical shift. The blue stick corresponds to isotactic and the pink stick to syndiotactic.

Except for H-4, good agreement can be seen between the observed and calculated chemical shifts for the relative chemical shifts of the isotactic and syndiotactic ^1H and ^{13}C NMR peaks of the dimer model compounds, irrespective of the quantum chemical methods or the basis sets. For H-4, the observed syndiotactic peak appears downfield from the isotactic peak, and this trend agrees with calculation codes (a), (d) and (g) in Figure 7. In these three calculations, (a), (d) and
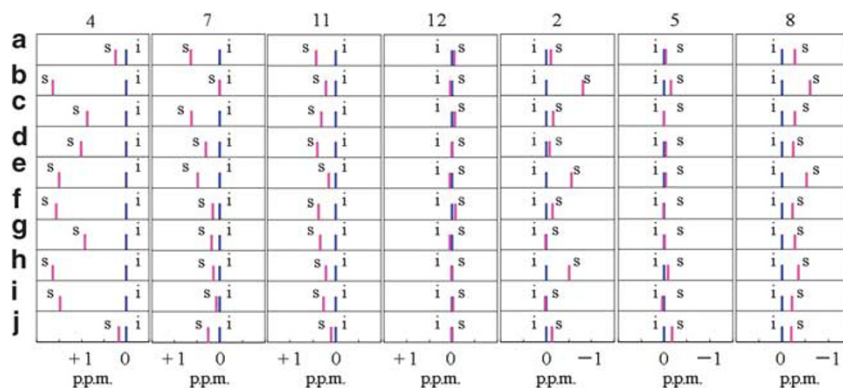
Figure 8 Comparison of the calculated and observed ^{13}C chemical shifts (in p.p.m.) of PLA dimer model compounds (**1**) shown as stick spectra. (a–i) represent the calculated chemical shift, (j) represents the observed chemical shift. The identity of each code is shown in row 3 of Tables 3 and 4. The chemical shifts are shown relative to the isotactic chemical shift. The blue stick corresponds to isotactic and the pink stick to syndiotactic.

(g), the method used to perform conformational optimization was B3LYP, and the method used to perform the chemical shift calculations of the preferred conformation was HF, although the basis sets were different. In general, the B3LYP method is effective in calculating the electron distribution state for the whole molecule, and HF is effective in calculating the local electron distribution state in the neighborhood of nuclei of interest. For H-4, the calculation codes (b), (e) and (h) in Figure 7 do not agree with the observed chemical shift. This discrepancy occurred because tacticity splitting in the NMR spectra depends on not only the electron distribution state in the whole molecule, but also the local electron distribution state. Similar reasoning applied to the calculation codes (c), (f) and (i) in Figure 7. Conformation depends on the electron distribution state in the whole molecule, and the chemical shift depends on the local electron distribution state in the neighborhood of nuclei of interest. Thus, B3LYP is preferred for conformational optimization, and HF is preferred for the chemical shift calculation. Note that B3LYP includes electron correlation in the calculation but only approximates it. Even better results would likely be obtained if the electron correlation were calculated exactly without resorting to approximations, but the computation time needed would be prohibitive. Moreover, the considerations made regarding the calculation methods used are not confined to the case of PLA. It is likely that the combination of HF and B3LYP, rather than the use of each method by itself, would also be preferred in studying other compounds.

In summary, satisfactory results for the calculated shifts of different tacticities of PLA dimer have been obtained in a comparatively short time by combining B3LYP with HF methods. The calculations suggest that the different electronic environments of ^{1}H and ^{13}C nuclei, their electron correlations and the conformation of the molecules contribute to the tacticity splitting in the NMR spectra of PLA and the PLA dimer model compounds.

1 Södergård, A. & Stolt, M. Properties of lactic acid based polymers and their correlation with composition. *Prog. Polym. Sci.* **27,** 1123–1163 (2002).
2 Garlotta, D. A literature review of poly(lactic acid). *J. Polym. Environ.* **9,** 63–84 (2001).
3 Filachione, E.M. & Fisher, C.H. Lactic acid condensation polymers. *Ind. Eng. Chem* **36,** 223–228 (1944).
4 de Jong, S.J., van Dijk-Wolthuis, W.N.E., Kettenes-van den Bosch, J.J., Schuyl, PJ.W. & Hennink, W.E. Monodisperse enantiomeric lactic acid oligomers: Preparation, characterization, and stereocomplex formation. *Macromolecules* **31,** 6397–6402 (1998).
5 Schliecker, G., Schmidt, C., Fuchs, S. & Kissel, T. Characterization of a homologous series of D,L-lactic acid oligomers; a mechanistic study on the degradation kinetics *in vitro*. *Biomaterials* **24,** 3835–3844 (2003).
6 Kaitian, X., Kozluca, A., Denkbas, E.B. & Piskin, E. Poly(D,L-lactic acid) homopolymers: Synthesis and characterization. *Tr. J. Chem.* **20,** 43–53 (1996).
7 Okamoto, K., Toshima, K. & Matsumura, S Degradation of poly(lactic acid) into repolymerizable oligomer using montmorillonite K10 for chemical recycling. *Macromol. Biosci.* **5,** 813–820 (2005).
8 de Jong, S.J., De Smedt, S.C., Wahls, M.W.C., Demeester, J., Kettenes-van der Bosch, J.J. & Hennink, W.E. Novel self-assembled hydrogels by stereocomplex formation in aqueous solution of enantiomeric lactic acid oligomers grafted to dextran. *Macromolecules* **33,** 3680–3686 (2000).
9 Burdick, J.A., Philpott, L.M. & Anseth, K.S. Synthesis and characterization of tetrafunctional lactic acid oligomers: a potential in situ forming degradable orthopedic biomaterial. *J. Polym. Sci. A Polym. Chem.* **39,** 683–692 (2001).
10 Hill, G.T.H., Irvine, D.J., Thurecht, K.J., Botting, C.H., Williamson, S. & Cole-Hamilton, D.J. Preparation of sodium-capped poly(lactic acid) oligomers by catalytic initiation with a sodium α-, β-, or γ-hydroxyacids. *Macromolecules* **43,** 185–192 (2010).
11 Coullerez, G., Lowe, C., Pechy, P., Kausch, H.H. & Hilborn, J. Synthesis of acrylate functional telechelic poly(lactic acid) oligomer by transesterification. *J. Mater. Sci. Mater. Med.* **11,** 505–510 (2000).
12 van den Berghe, H., Coudane, J. & Vert, M. Isocyanate-terminated lactic acid oligomers as a new means to conjugate functional drugs or polymers with bioresorbable hydrophobic segments. *J. Bioact. Comp. Polym.* **22,** 637–650 (2007).
13 Perego, G., Cella, G.D. & Bastioli, C. Effect of molecular weight and crystallinity on poly(lactic acid) mechanical properties. *J. Appl. Polym. Sci.* **59,** 37–43 (1996).
14 Coupin, T., Coszach, P. & Hottois, D. Isotactic polylactic acid and method for producing same. *US Patent Appl.* 20110319588.
15 Shaver, M.P. & Cameron, D.J.A. Tacticity control in the synthesis of poly(lactic acid) polymer stars with dipentaerythritol cores. *Biomacromolecules* **11,** 3673–3679 (2010).
16 Cameron, D.J.A. & Shaver, M.P. Control of thermal properties and hydrolytic degradation in poly(lactic acid) polymer stars through control of isospecificity of polymer arms. *J. Polym. Sci. A Polym. Chem* doi:10.1002/pola.25927.
17 Okihara, T., Tsuji, M., Kawaguchi, A. & Katayama, K. Crystal structure of stereocomplex of poly(L-lactide) and poly(D-lactide). *J. Macromol. Sci. Phys.* **B30,** 119–140 (1991).
18 Ikada, Y., Jamshidi, K., Tsuji, H. & Hyon, S.-H. Stereocomplex formation between enantiomeric poly(lactides). *Macromolecules* **20,** 904–906 (1987).
19 Tsuji, H. & Ikada, Y. Stereocomplex formation between enantiomeric poly(lactic acids). 9. Stereocomplexation from the melt. *Macromolecules* **26,** 6918–6926 (1993).
20 Tsuji, H. & Ikada, Y. Stereocomplex formation between enantiomeric poly(lactic acid)s. 6. Binary blends from copolymers. *Macromolecules* **25,** 5719–5723 (1992).
21 Li, L., Zhong, Z., de Jeu, W.H., Dijkstra, P.J. & Feijen, J. Crystal structure and morphology of poly(L-lactide-b-D-lactide) diblock copolymers. *Macromolecules* **37,** 8641–8646 (2004).
22 Fukushima, K. & Kimura, Y. A novel synthetic approach to stereo-block poly(lactic acid). *Macromol. Symp.* (2005)**224,** 133–143.

23 Fukushima, K., Furuhashi, Y., Sogo, K., Miura, S. & Kimura, Y. Stereoblock poly(lactic acid): synthesis via solid-state polycondensation of a stereocomplexed mixture of poly(L-lactic acid) and poly(D-lactic acid). *Macromol. Biosci.* **5,** 21–29 (2005).

24 Bero, M., Kasperczyk, J. & Jedlinski, Z. J. Coordination polymerization of lactides, 1. Structure determination of obtained polymers. *Makromol. Chem.* **191,** 2287–2296 (1990).

25 Kricheldorf, H.R., Boettcher, C. & Tonnes, K. Polylactones: 23. polymerization of *racemic* and *meso* D,L-lactide with various organotin catalysts-stereochemical aspects. *Polymer* **33,** 2817–2824 (1992).

26 Kasperczyk, J.E. Microstructure analysis of poly(lactic acid) obtained by lithium tert-butoxide as initiator. *Macromolecules* **28,** 3937–3939 (1995).

27 Thakur, K.A.M., Kean, R.T. & Hall, E.S. High-resolution ^{13}C and ^{1}H solution NMR study of poly(lactide). *Macromolecules* **30,** 2422–2428 (1997).

28 Kasperczyk, J.E. HETCOR NMR study of poly(*rac*-lactide) and poly(*meso*-lactide). *Polymer* **40,** 5455–5458 (1999).

29 Chisholm, M.H., Iyer, S.S., McCollum, D.G., Pagel, M. & Werner-Zwanziger, U. Microstructure of poly(lactide). phase-sensitive HETCOR spectra of poly(meso-lactide), poly(rac-lactide), and atactic poly(lactide). *Macromolecules* **32,** 963–973 (1999).

30 Zell, M.T., Padden, B.E., Paterick, A.J., Thakur, K.A.M., Kean, R.T., Hillmyer, M.A. & Munson, E.J. Unambiguous determination of the ^{13}C and ^{1}H NMR stereosequence assignments of polylactide using high-resolution solution NMR spectroscopy. *Macromolecules* **35,** 7700–7707 (2002).

31 Suganuma, K., Horiuchi, K., Matsuda, H., Cheng, H.N., Aoki, A. & Asakura, T. Stereoregularity of poly(lactic acid) and their model compounds as studied by NMR and quantum chemical calculations. *Macromolecules* **44,** 9247–9253 (2011).

32 Bax, A. & Subramanian, S. Sensitivity-enhanced two-dimensional heteronuclear shift correlation NMR spectroscopy. *J. Magn. Reson.* **67,** 565–569 (1986).

33 Bax, A. & Summers, M.F. [1]H and [13]C Assignments from sensitivity-enhanced detection of heteronuclear multiple-bond connectivity by 2D multiple quantum NMR. *J. Am. Chem. Soc.* **108,** 2093–2094 (1986).

34 Summers, M.F., Marzilli, L.G. & Bax, A. Complete proton and carbon-13 assignments of coenzyme B12 through the use of new two-dimensional NMR experiments. *J. Am. Chem. Soc.* **108,** 4285–4294 (1986).

35 Carbone, P., Ragazzi, M., Tritto, I., Boggioni, L. & Ferro, D.R. Ab initio molecular modeling of ^{13}C NMR chemical shifts of polymers. 2. propene−norbornene copolymers. *Macromolecules* **36,** 891–899 (2003).

36 Boggioni, L., Bertini, F., Zannoni, G., Tritto, I., Carbone, P., Ragazzi, M. & Ferro, D. R. Propene-norbornene copolymers: synthesis and analysis of polymer structure by ^{13}C NMR spectroscopy and ab initio chemical shift computations. *Macromolecules* **36,** 882–890 (2003).

37 Wu, W., Li, W., Wang, L., Zhang, P. & Zhang, J. Density functional theory study on lactides: geometries, IR, NMR and electronic spectra. *Theochem.* **816,** 13–19 (2007).

38 Kang, Y.K. & Byun, B. Conformational preferences and cis-trans isomerization of L-lactic acid residue. *J. Phys. Chem. B* **112,** 9126–9134 (2008).

39 Inai, Y. & Ogawa, H. [Theoretical studies on conformational features of poly(lactic acid) chain containing a racemic unit]. *Kobunshi Ronbunshu* **67,** 214–223 (2010).

40 McAliley, J.H., O'Brien, C.P. & Bruce, D.A. Continuum electrostatics for electronic structure calculations in bulk amorphous polymers: application to polylactide. *J. Phys. Chem. A* **112,** 7244–7249 (2008).

41 Sadlej, J., Dobrowolski, J.C., Rode, J.E. & Jamroz, M.H. DFT study of vibrational circular dichroism spectra of D-lactic acid water complexes. *Phys. Chem. Chem. Phys.* **8,** 101–113 (2006).

42 Becke, A.D. Density-functional thermochemistry. III. The role of exact exchange. *J. Chem. Phys.* **98,** 5648 (1993).

43 Dickinson, B.N. The normal state of the hydrogen molecule-ion. *J. Chem. Phys.* **1,** 317 (1933).

44 Frisch, M.J., Pople, J.A. & Binkley, J.S. Self-consistent molecular orbital methods 25. supplementary functions for gaussian basis sets. *J. Chem. Phys.* **80,** 3265 (1984).

45 Clark, T., Chandrasekhar, J., Spitznagel, G.W. & Schleyer, P.v.R. Efficient diffuse function-augmented basis sets for anion calculations. III. The 3-21 + G basis set for first-row elements, Li–F. *J. Comp. Chem.* **4,** 294–301 (1983).

46 Schafer, A., Horn, H. & Ahlnichs, R. Fully optimized contracted Gaussian basis sets for atoms Li to Kr. *J. Chem. Phys.* **97,** 2571–2577 (1992).

47 Schafer, A., Huber, C. & Ahlnichs, R. Fully optimized contracted Gaussian basis sets of triple zeta valence quality for atoms Li to Kr. *J. Chem. Phys.* **100,** 5829–5835 (1994).

48 Becke, A.D. Density-functional thermochemistry. III. The role of exact exchange. *J. Chem. Phys.* **98,** 5648–5652 (1993).

49 Woon, D.E. & Dunning, Jr. T.H. Gaussian basis sets for use in correlated molecular calculations. III. The atoms aluminum through argon. *J. Chem. Phys.* **98,** 1358–1371 (1993).

50 Kendall, R.A., Dunning, Jr. T.H. & Harrison, R.J. Electron affinities of the first-row atoms revisited. Systematic basis sets and wave functions. *J. Chem. Phys.* **96,** 6796–6806 (1992).

51 Dunning, Jr. T.H. Gaussian basis sets for use in correlated molecular calculations. I. The atoms boron through neon and hydrogen. *J. Chem. Phys.* **90,** 1007–1023 (1989).

52 Peterson, K.A., Woon, D.E. & Dunning, Jr. T.H. Benchmark calculations with correlated molecular wave functions. IV. The classical barrier height of the $H+H_2 \rightarrow H_2+H$ reaction. *J. Chem. Phys.* **100,** 7410–7415 (1994).

53 Wilson, A.T., Mourik, T.V. & Dunning, Jr. T.H. Gaussian basis sets for use in correlated molecular calculations. VI. Sextuple zeta correlation consistent basis sets for boron through neon.. *J. Mol. Struct. (Theochem)* **388,** 339–349 (1996).

54 London, F. [Théorie quantique des courants interatomiques dans les combinaisons aromatiques]. *J. Phys. Radium* **8,** 397–409 (1937).

55 McWeeny, R. Perturbation theory for the Fock-Dirac density matrix. *Phys. Rev.* **126,** 1028–1034 (1962).

56 Ditchfield, R. Self-consistent perturbation theory of diamagnetism I. A gauge- invariant LCAO method for N.M.R. chemical chifts. *Mol. Phys.* **27,** 789–807 (1974).

57 Wolinski, K., Hilton, J. F. & Pulay, P. Efficient implementation of the gauge-independent atomic orbital method for NMR chemical shift calculations. *J. Am. Chem. Soc.* **112,** 8251–8260 (1990).

58 Cheeseman, J.R., Trucks, G.W., Keith, T.A. & Frisch, M.J. A comparison of models for calculating nuclear magnetic resonance shielding tensors. *J. Chem. Phys.* **104,** 5497–5509 (1996).